2-24-2010

On the anomalous balmer line strengths in globular clusters

Violet Poole

Guy Worthey

Hyun Chul Lee

Jedidiah Serven

Recommended Citation

ON THE ANOMALOUS BALMER LINE STRENGTHS IN GLOBULAR CLUSTERS

Violet Poole, Guy Worthey, Hyun-chul Lee, and Jedidiah Serven
Department of Physics and Astronomy, Washington State University, Pullman, WA 99163, USA; gworthey@wsu.edu

ABSTRACT

Spectral feature index diagrams with integrated globular clusters and simple stellar population models often show that some clusters have weak Hβ, so weak that even the oldest models cannot match the observed feature depths. In this work, we rule out the possibility that abundance mixture effects are responsible for the weak indices unless such changes operate to cool the entire isochrone. We discuss this result in the context of other explanations, including horizontal branch morphology, blue straggler populations, and nebular or stellar emission fill-in, finding a preference for flaring in M giants as an explanation for the Hβ anomaly.

Key words: blue stragglers – globular clusters: general – stars: abundances – stars: flare – stars: horizontal-branch

Online-only material: color figures

1. INTRODUCTION

Globular clusters are often the only objects that can be detected in the halos of other galaxies. Since most globular clusters are very old, studying them provides vital information about the formation and chemical history of these galaxies (Gratton et al. 2004). The similar ages of the constituent stars and low velocity dispersion make these objects relatively easy to study in integrated light.

The most reliable way to obtain information about age and abundance patterns of a stellar population is star-by-star analysis via a color–magnitude diagram (CMD). However, this technique is only feasible for nearby objects, due to the limits of current instrumentation. Therefore, we need to develop reliable methods for analyzing the composite light from all the stars in these systems. This is no easy feat, since many factors can complicate the analysis.

One of the biggest problems that plagues the study of the integrated light of a stellar population is the very similar effects that age and metallicity have on the spectra of stellar populations (O'Connell 1986). However, the degeneracy between the age and metallicity can be broken. Rabin (1980, 1982) and Gunn et al. (1981) noticed that the Balmer lines are quite sensitive to age. Combining this with the knowledge that metal lines, such as Mg b, [MgFe], or ⟨Fe⟩, are relatively more sensitive to metallicity than age (Worthey 1994), the degeneracy between age and metallicity can be broken by plotting the strength of the Balmer lines versus metallic absorption blends. This is because Hβ operates in such a way that its strength is nonlinear with temperature, especially between 6000 K and 9000 K, where main-sequence turnoff stars from a few hundred megayears to ancient reside. But stars of other kinds also inhabit that temperature band.

The Hβ-metal-index grids give the impression that age and metallicity are the only factors that affect a population's location in the grid, but of course this is misleading. As you can see from Figure 1(a), other factors must be affecting the values of the indices, since they are quite scattered and some are off the grid. For comparison, an average of the Virgo elliptical galactic nuclei is also plotted along with the globular cluster data (J. Serven et al. 2010, in preparation).

Observational difficulties play a main role, of course. There are sometimes horizontal branch (HB) and blue straggler stars that can contribute enough to alter the line strengths. Rarer stars such as asymptotic giant branch (AGB)-Manque stars (Greggio & Renzini 1990) and planetary nebulae can be ruled out as being significant contributors under ordinary circumstances, as can the much fainter white dwarf population. These warm stars make the Balmer indices stronger, not weaker, so for populations of these stars to represent a "solution" to the mystery, there would also need to be a systematic error in the models to weaken Balmer index strength.

Additionally, there is the possibility that Hβ is being filled in by nebular emission from hydrogen recombination lines. This fill-in could come from diffuse gas, but it could also come from flaring stars of various sorts; AGB stars, M-type dwarfs, cataclysmic variables, and others are known to have transient emission-line spectra (Schiavon et al. 2005).

Finally, there is the possibility that abundance-mixture effects could drive a significant change in Hβ and other feature strengths. This is a relatively unexplored avenue of investigation, but the tools now exist to probe the question (Dotter et al. 2007; Lee et al. 2009), and that is our primary task in this paper.

The models and observational data are already available in the literature, but the implementation is recapped in Section 2. The implications of our investigation are discussed in Section 3, and then there is a brief conclusion.

2. OBSERVATIONS AND MODELS

A version of integrated-light models (Worthey 1994; Trager et al. 1998) that use a new grid of synthetic spectra in the optical (Lee et al. 2009) in order to investigate the effects of changing the detailed elemental composition on an integrated spectrum was used to create synthetic spectra at a variety of ages and metallicities for single-burst stellar populations. The underlying isochrones for most of the present paper were the Worthey (1994) ones, because they allow us "manual" HB morphology control. However, there are certain caveats to using these isochrones. Specifically, the models are a bit crude by today's standards and the ages are about 2 Gyr too old, so that 17 Gyr should really be interpreted as 15 Gyr. Other isochrone sets were used to check the results.

For this exercise, new stellar index fitting functions were generated. The data sources include a variant of the original Lick collection of stellar spectra (Worthey et al. 1994) in which the
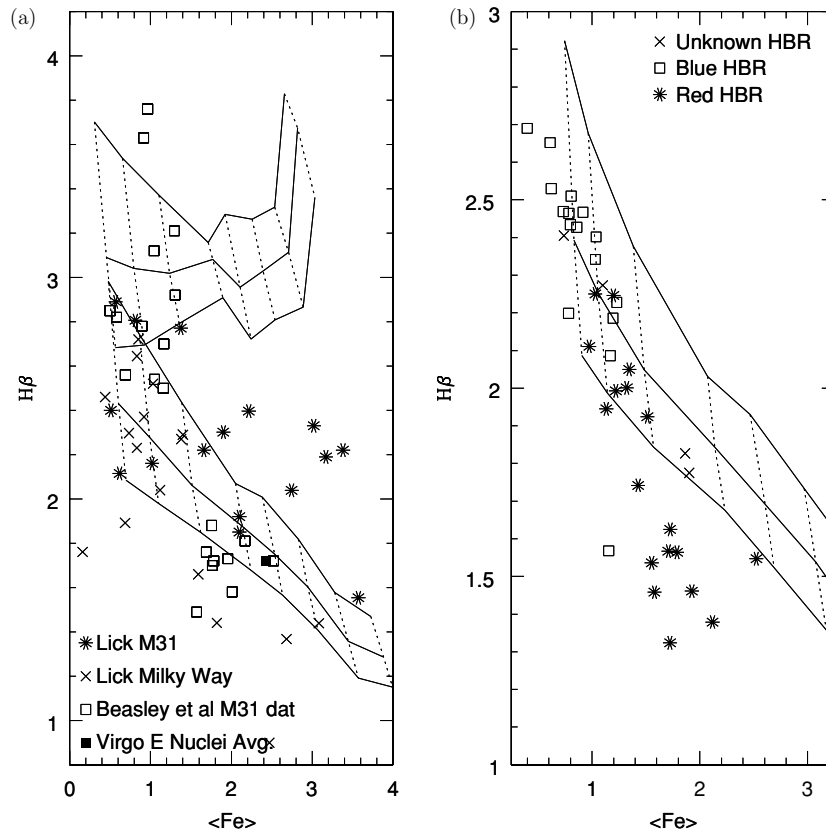
Figure 1. (a) Literature data for Lick indices plotted for globular clusters in the Milky Way and M31 (Trager et al. 1998; Beasley et al. 2005). Also plotted is an average of the Virgo elliptical galactic nuclei (J. Serven et al. 2010, in preparation). Two model grids (Worthey & Ottaviani 1997) are shown in this figure. The lower one has a forced red clump morphology for the HB, while the top grid has all hot HB stars. Even using different models, we still have the problem that some globular clusters are weaker in Hβ than the reddest models, appearing much older than could be realistic. (b) Hβ and ⟨Fe⟩ indices for globular clusters (from Schiavon et al. 2005) and models. Horizontal lines are models with ages: 8, 12, and 17 Gyrs from top to bottom. Vertical lines are models at different metallicities. Globular clusters are plotted on the same graph, divided into two groups. Red HBR have $X_{HB} = (B − R)/(B + V + R)$ greater than zero, while Blue HBR type have X_{HB} less than zero. Both of the pair of Fe-strong blue X's (NGC 6388, NGC 6441) are known to have a partially blue HB (Busso et al. 2007). The uncertainty is smaller than the point size used to plot the data.

wavelength scale of each observation has been refined via cross-correlation, as well as the MILES spectral library (Sanchez-Blazquez et al. 2007) with some zero-point corrections, and the Coude Feed library (CFL) of Valdes et al. (2004). The CFL was used as the fiducial set, in the sense that any zero-point shifts between libraries were corrected to agree with the CFL case. The MILES and CFL spectra were smoothed to a common Gaussian smoothing corresponding to 200 km s^{-1}. The rectified Lick spectra were measured and then a linear transformation was applied to put it on the fiducial system.

Multivariate polynomial fitting was done in five overlapping temperature swaths as a function of $\theta_{eff} = 5040/T_{eff}$, log g, and [Fe/H]. The fits were combined into a lookup table for final use. As in Worthey (1994), an index was looked up for each "star" in the isochrone and decomposed into "index" and "continuum" fluxes, which added, then re-formed into an index representing the final, integrated value after the summation. This gives us empirical index values. After that, additive index deltas were applied as computed from the grid of new synthetic spectra when variations in chemical composition are needed. The grid of synthetic spectra is complete enough to predict nearly arbitrary composition changes.

We also smoothed the Schiavon et al. (2005) globular cluster spectra to 200 km s^{-1} or the Lick (Worthey & Ottaviani 1997) resolution, as needed, and measured Lick or Lick-like pseudo-equivalent width indices (Worthey et al. 1994; Worthey

& Ottaviani 1997; Serven et al. 2005) from them. When the globular clusters and the age–metallicity model grid of values are plotted on the same graph (see Figures 1(b) and 2) a globular cluster's position in the grid allows one to estimate its age and metallicity, at least naively.

Cursory examination of these graphs yields a puzzling thing. On graphs with Hβ as one of the indices, some of the globular clusters lie much below the oldest age plotted for 17 Gyr (see Figure 1(a)). However, graphs that are not plotted with the Hβ index as one of the axes do not have this problem (see Figure 2). This indicates that there could be something going on in the spectra of these globular clusters near the Hβ line that does not affect Hγ or Hδ to the same degree. It could also indicate that the models for the Hβ index are not correct.

3. DISCUSSION: BALMER FEATURES IN THE INTEGRATED LIGHT OF GLOBULAR CLUSTERS

Many factors could potentially affect the Balmer features in the integrated light of the globular clusters. We consider effects due to abundance ratios, HB morphology, the presence of blue stragglers, and emission fill-in of the Balmer lines due to hydrogen recombination lines from either external nebulae or stellar activity in individual cluster stars. We also consider the illusions due to miscalibrated models.
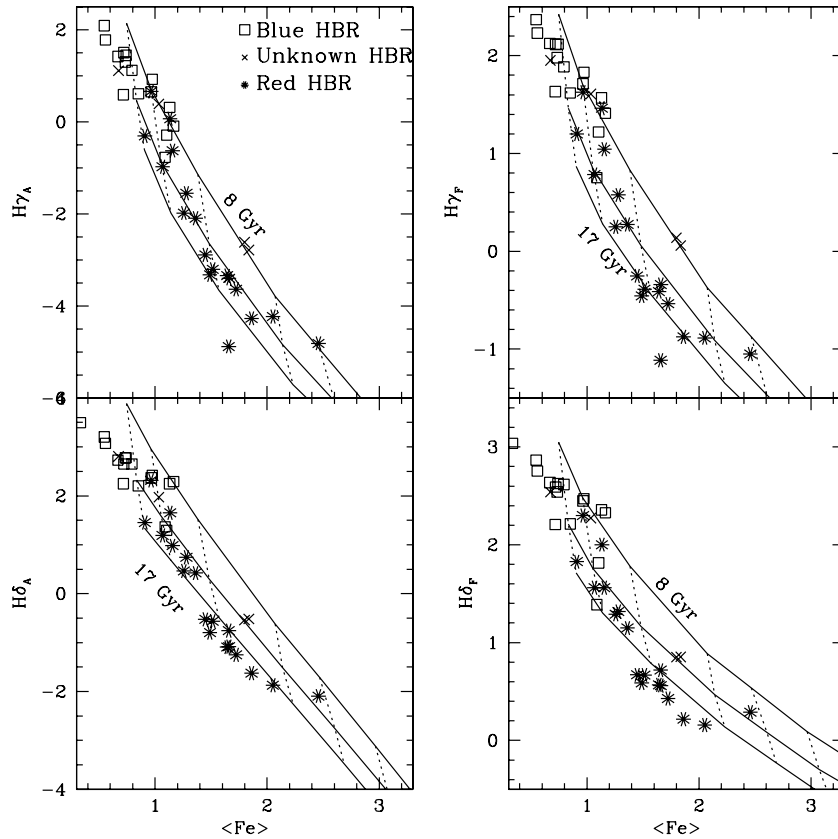
Figure 2. (a) Hγ_A vs. $\langle$Fe$\rangle$ for globular clusters and models. (b) Hγ_F vs. $\langle$Fe$\rangle$ for globular clusters and models. (c) Hδ_A vs. $\langle$Fe$\rangle$ for globular clusters and models. (d) Hδ_F vs. $\langle$Fe$\rangle$ for globular clusters and models. The meanings of lines and symbols are the same as in Figure 1(a).

3.1. Abundance Ratio Effects

It is of interest to examine the spectra themselves for evidence to support the various hypotheses that could explain their behavior. Comparison of the spectra of the globular clusters with ages off the grid to the spectra of globular clusters with similar metallicity lying within the grid indicates that the main difference is the depth of the Hβ line itself, rather than a difference in heights of either the blue or red continuum bands (see Figure 3). Specifically, the Hβ lines of the clusters off the grid are shallower than those that are on the grid, and, morphologically, this does not seem to be a problem in the continuum regions at all, but a true modulation of the Hβ line itself.

Figure 3 should be compared to Figure 4, which shows several model population spectra with [X/R] = 0.3 dex, where X stands for Fe, Mg, Ti, or Ni, and R stands for "generic heavy element." Other simple element variations from solar were explored, but these four had the largest impact on the spectrum shape. We note that none of the elements affect the model depth of the Hβ line itself and have only modest effects in the continuum regions. Visually, Fe enhancement raises the average height of the red continuum band. Quantitatively, however, this "extra slope" does little to change the actual index value. Furthermore, in comparing model spectra with the observed globular cluster spectra, raising the red continuum flux does not improve the appearance of the spectral match.

A more quantitative way to analyze the effect due to element enhancement is by looking at the spectral response of the indices when the various elements are enhanced in the same way as Serven et al. (2005). The results of these calculations on our
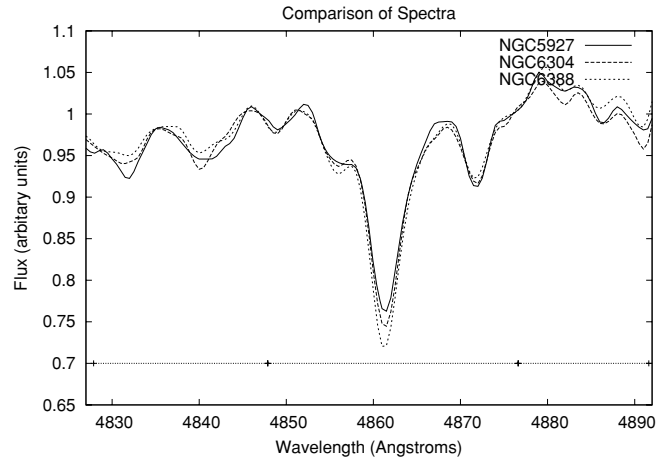

Figure 3. Comparison of the spectra of globular clusters at approximately the same metallicity. NGC 6388 appears on the age–metal grid while NGC 5927 and NGC 6304 are below the grid, and the stronger Hβ feature is obvious.

model spectra can be found in Table 1. Row 1 is the model index while row 2 is the uncertainty assuming a signal-to-noise ratio (S/N) = 100 at 5000 Å. Rows 3–25 list the change of index when the labeled element is enhanced by 0.3 dex, while the last row has all elements up by 0.3 dex. As one can see, most elements have little effect on the Hβ index. Two iron-peak elements, Fe and Ni, oppose each other in the sign of their effects, and two alpha elements, Mg and Ti, oppose each other in the sign of their effects. If the alpha elements and the iron-peak elements internally rise or fall together, then Hβ is basically completely clean from spectral effects from element
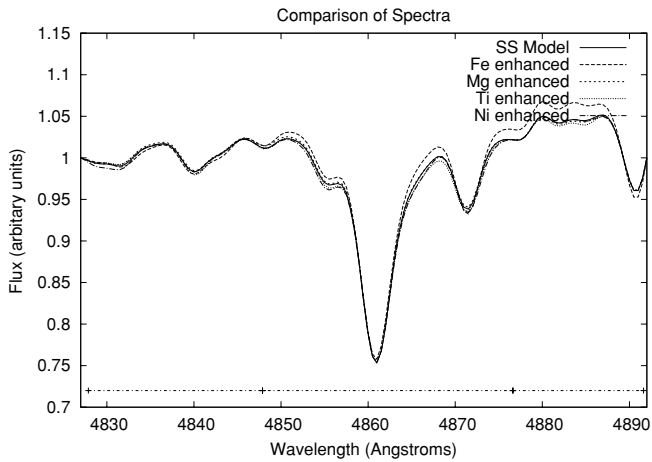
Figure 4. Comparison of model spectra near the Hβ line, with various element enhancements. SS refers to scaled-solar, and the rest are enhanced by 0.3 dex, element by element, with total heavy element abundance held constant.

Table 1
Spectral Response of Indices Under Various Element Enhancements

	Hβ	Hδ_F	Hγ_F	Mg$_b$	Fe5270	Fe5335
I_{OB}	1.522	0.613	−0.709	2.121	2.025	1.762
Error	0.138	0.119	0.121	0.155	0.173	0.199
C	0.00	−0.16	−4.17	−0.19	0.16	0.06
N	0.00	−0.04	−0.03	−0.01	0.06	0.01
O	0.04	−0.11	0.76	0.12	−0.04	−0.01
Na	0.01	−0.01	0.07	−0.09	−0.03	−0.03
Mg	−0.29	0.16	1.12	4.83	−0.32	−0.26
Al	0.02	0.01	0.11	−0.06	−0.05	−0.05
Si	0.07	1.88	0.79	−0.32	−0.09	−0.07
S	0.00	0.00	0.01	0.00	0.00	0.00
K	0.00	0.00	0.01	0.00	−0.01	−0.01
Ca	−0.02	0.56	−0.21	0.06	0.06	0.03
Sc	−0.01	−0.03	−0.27	0.00	−0.14	0.03
Ti	0.28	−0.54	−0.10	0.01	0.28	0.14
V	−0.02	0.53	−0.02	−0.02	−0.05	0.01
Cr	−0.12	0.03	0.66	−0.86	0.10	0.39
Mn	−0.02	−0.41	−0.04	−0.09	0.09	0.04
Fe	−0.57	−2.62	−0.85	−0.79	1.88	1.54
Co	−0.02	−0.21	−0.01	0.00	0.13	0.16
Ni	0.61	−0.09	−0.11	0.00	0.06	0.00
Cu	0.00	0.00	0.00	−0.07	−0.01	0.00
Zn	0.00	0.00	0.00	0.00	0.00	0.00
Sr	0.00	−0.34	0.00	0.00	0.00	0.00
Ba	0.00	−0.06	0.00	0.00	0.00	0.00
Eu	0.00	−0.06	0.00	0.00	0.00	0.00
UpX2	0.09	1.95	2.31	4.48	0.45	−0.21

Notes. Row 1 is the model index, row 2 is the uncertainty assuming an S/N = 100 at 5000 Å, rows 3–25 list the change of index when the labeled element is enhanced by 0.3 dex, and the last row has all elements up by 0.3 dex.

enhancement. This is in broad agreement with observations made directly from the model spectra.

Parenthetically, Table 1 does not show similar cleanliness for any other index, with Mg b responding to Mg, Fe indices responding to Fe, Hδ responding to Fe and Si, and Hγ responding to C, O, Mg, Si, Cr, and Fe!

The lack of signal in the Hβ index seems to indicate that the reason for larger spread in ages for grid with the Hβ index as one of the axes is most likely not due to enhancement of one element or any group of elements that directly change the spectral shapes. There remains, perhaps, a possibility of
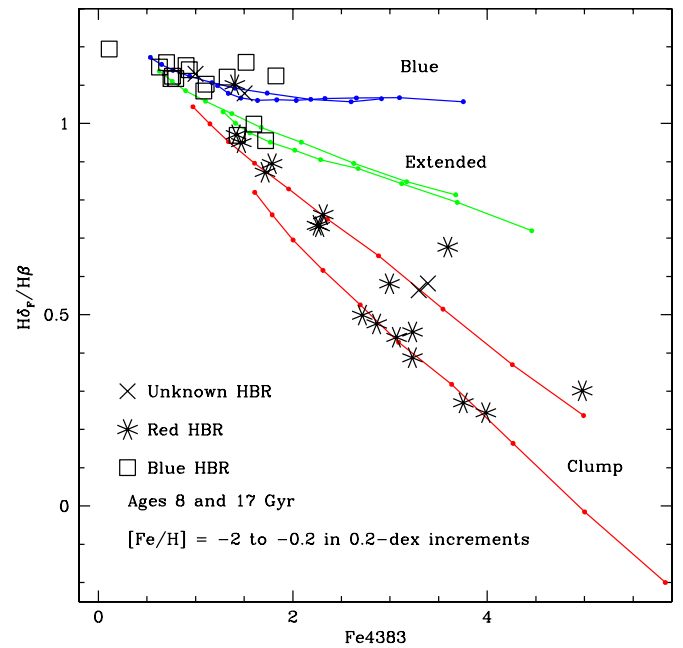

Figure 5. Balmer index ratio vs. Fe4383, a HB diagnostic diagram. Worthey (1994) Models for ages 8 and 17 Gyrs between [Fe/H] −2 and −0.2 are plotted in increments of 0.2 dex. The upper sequence has a HB morphology that is forced to be blue. The middle sequence represents a HB extended in temperature. The lower sequences represents a red clump morphology. Symbols for globular cluster data are as in previous figures.

(A color version of this figure is available in the online journal.)

elements that do not make direct spectral changes, but might affect the temperatures of the stars as a whole, such as O and the noble gases He and Ne. An excess of O or a dearth of He would make the isochrones, at least, around the main-sequence turnoff region of the H–R diagram, cooler. If metal-rich globular clusters tend to have such a mixture, but elliptical galaxies do not, then it may work out as observed, but of course there is no reason to suspect a chemical bifurcation in the two classes of metal-rich stellar populations.

3.2. Horizontal Branch Morphology

Horizontal branch morphology, that is "red clump," "extended," "blue," or "extreme," is easy to determine with a good CMD of the stars within the globular cluster, but difficult to disentangle via integrated-light measures because of significant degeneracy with both age and metallicity (cf. Figure 37 of Worthey 1994). Blue HB morphology can increase the Hβ index by as much as 0.75 Å compared to clump (Lee et al. 2000). Figure 1(a) illustrates how different HB morphology can shift the model grids by showing two model grids with different HB morphologies. This shift gives the appearance that the globular clusters with blue HB morphologies are younger or more metal poor than they really are.

Schiavon et al. (2004) proposed that the ratio of Hδ_f/Hβ is more sensitive to HB morphology than to age allowing us to break the degeneracy present between these two parameters. Graphs with Hδ_f/Hβ versus iron indices have globular clusters with mostly blue HB morphologies that appear displaced relative to the locus occupied by the models, as shown in Figure 5. Since in the Milky Way globular cluster system, the HB morphology changes from blue to red at around [Fe/H] = −1, there is some ambiguity with metallicity.
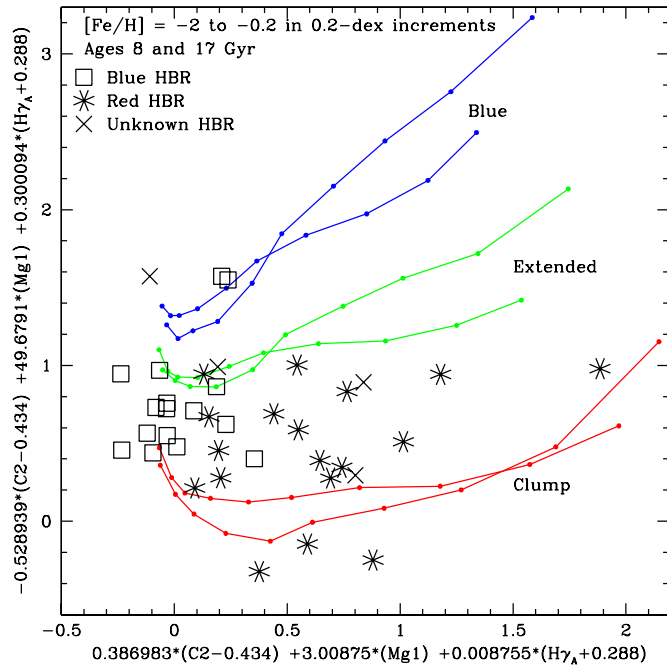
Figure 6. Example of a diagnostic index combination plot that attempts to separate HB morphology (y-axis) and metallicity (x-axis). Model sequences are as in Figure 5.

(A color version of this figure is available in the online journal.)

It is unlikely that a ratio of Balmer indices will be completely optimal for detecting an extended HB. Indeed, we know of no effort to optimize the integrated-light detection of HB types in the literature, so we provide a simple one in this work. The idea is to pick three indices, and force them to provide solutions for age, HB morphology, and metallicity—three equations in three unknowns. The models used as a base are the Worthey (1994) models because the HB can be forced to be clump, extended, or blue at any metallicity. Then an error assigned to each color, magnitude, or index yields a propagated error in age, morphology, or abundance.

The corners used for the linearization are ages 11 Gyr and 17 Gyr, [Fe/H] of −1.8 and −0.6, and morphologies either red clump or blue, where clump was assigned a numerical value of 0, and blue a numerical value of 1. The models also come in an "extended" HB morphology that stretches from the red clump to $\log T_{\mathrm{eff}} = 4.0$, but in this paper we only use those models for plots. The "blue" morphology has stars between $\log T_{\mathrm{eff}} = 3.9$ and $\log T_{\mathrm{eff}} = 4.1$. Errors were assigned to each index, and then used to do error propagation in the linear solutions, giving a goodness of fit for age, morphology, and metallicity.

An example of this is shown in Figure 6. For each trio of indices, the HB solution is on the y-axis, and the metallicity solution is on the x-axis. Model sequences for ages 8 Gyr and 17 Gyr are shown at 0.2 dex intervals from [Fe/H] = −2.0 to −0.2, and the collection of Schiavon et al. (2004) indices is shown, symbols varying between HBR < 0 and HBR > 0, as in previous figures. In the figure, the model sequences separate much more than the simpler Balmer index ratio plot. However, we caution that the models used are rather out of date, and better solutions might be found from more up-to-date isochrones.

In terms of HB morphology being responsible for the too-low Hβ strengths, this hypothesis seems doomed. The models that do not match already have the reddest possible HB morphology, and the models fit both blue and red HBs for most clusters, just not the anomalous group of redder clusters.

3.3. Blue Stragglers

No provision for blue straggler stars is in the synthesis models. If such stars were present in the models, the Balmer line strengths would strengthen by several tenths of Å, in a sense to make the low-lying globular clusters lie even lower.

3.4. Emission Fill-in

Filling in of the absorption lines due to emission could change the depth of the lines present in the spectra. This change in depth will lower the Lick/IDS index value of the object which is what we want. Emission could be caused by many things, such as: gas clouds in the line of sight, planetary nebulae, supernova remnants, M dwarfs with active chromospheres, and AGB-type stars.

For example, if we adopt a star formation region like recombination spectrum for an optically thick nebula of 10^4 K and 10^4 electrons per cubic centimeter, Osterbrock (1989) gives the relative Balmer line intensities of $j\gamma/j\beta = 0.469$ and $j\delta/j\beta = 0.260$. For a given Hβ index fill-in value, the equivalent widths of the Hγ and Hδ indices can be predicted after correcting for (1) underlying continuum shape and (2) the widths of the indices themselves. Using values of $F_{c,\gamma}/F_{c,\beta} = 0.84$ and $F_{c,\delta}/F_{c,\beta} = 0.81$ for the relative continuum flux ratios, a 1 Å fill-in of Hβ propagates to fill-ins for the higher-order indices of $\Delta H\gamma_F = 0.76$ Å, $\Delta H\gamma_A = 0.37$ Å, $\Delta H\delta_F = 0.44$ Å, and $\Delta H\delta_A = 0.24$ Å.

Planetary nebulae can be seen, one by one, in Milky Way globular clusters, and only M5 has a planetary nebula, so they should be rare in M31 globular clusters as well. Supernova remnants are much more improbable. Gas clouds containing neutral sodium are known to exist along most lines of sight out of the galaxy (Bica & Alloin 1986) but there is no reason to expect ionized hydrogen to linger in the potential wells of globular clusters since the rms velocity for a 10,000 K proton is $v_{\mathrm{rms}} = (3kT/m)^{1/2} \sim 15$ km s^{-1} exceeds the escape velocity of all but the largest globular clusters. We thus discount these three explanations in general, keeping in mind that specific globular clusters can be affected this way.

However, the stellar sources are less easy to discount. We discuss active cool dwarfs and flaring giants together, although they are treated separately. M dwarfs are known to have active chromospheres, although old ones get less active (West et al. 2010). In addition, Schiavon et al. (2005) observed a probable bright, red giant flaring in their spectra. This star is bright enough so that, by itself, it will alter the integrated Balmer line strengths. The character of these two sources is different, however, in that the numerous M dwarfs are spatially broad and should be nearly constant in Balmer emission output while the giants are spatially discrete, and should be highly time variable. M dwarf light will still give a net Balmer emission signal because the M dwarfs are concentrated toward the center of the cluster, albeit less so than the more massive stars. In support of cool giants causing fill-in, the most metal-poor clusters do not have very cool giants. It is only at [Fe/H] ≈ −1 and above that clusters begin to have long-period variables and genuine M-type giants, and these are the clusters that show the anomalously low Hβ strengths.

Under some extreme assumptions, we use our models and the data of Kafka & Honeycutt (2006) to estimate the contribution of the emission of active M dwarfs. The Cohen et al. (1998) definition of Hα is output by our models. The Kafka & Honeycutt (2006) definition is somewhat different, but of course quite similar. For cooler M dwarfs, the index itself

Table 2
Δ Balmer Indices for Active M Dwarf Experiment as a Function of [Fe/H]

[Fe/H]	ΔHα	ΔHβ
−2.0	0.013	0.004
−1.5	0.021	0.006
−1.0	0.033	0.010
−0.5	0.155	0.056
0.0	0.307	0.126
0.5	0.278	0.131

Notes. The model sequence is for a 10 Gyr age simple stellar population. The IMF was set to a power law with a lower mass cutoff of 0.1 $M_\odot$. This plus the assumption that every dwarf with $\Theta > 0.42$ is highly active both will tend to exaggerate the effects of including active M dwarfs. The Hα definition used is that of Cohen et al. (1998) and the Hβ definition is that of Worthey et al. (1994).

goes negative (emission like) due to TiO absorption, and we were able to confidently trace the non-active envelope in the Kafka & Honeycutt (2006) data, and then assign an apparent turn-on temperature of 3600 K, and a ballpark "fully active" ΔHα ≈ −4.0 Å of equivalent width. Assuming that 100% of the stars cooler than 3600 K were fully active, we recalculated the models. We also assumed that the initial mass function (IMF) was a power law all the way to a cutoff of 0.1 $M_\odot$, which makes the coolest dwarfs more important in integrated light than direct counting suggests. The Hα and inferred Hβ results are listed in Table 2 as a function of metallicity.

The ΔHβ values in Table 2, even inflated as they are, are still short of the approximately 0.5 Å needed to come close to solving our Hβ dilemma, but the generic behavior is interesting, namely that metal-poor populations have so few stars that cool that the emission is completely negligible, but then the metal-rich populations, as judged by the last entry in the table, seem to saturate or plateau (because more and more non-active but cool stars contribute to the flux). This leads to a sort of on or off state, with "on" happening for old populations more metal rich than about −0.5 dex in [Z/H].

This tends to lend support to the cool-giant hypothesis, since they would share a similar gross temperature behavior with metallicity as do the dwarfs, and the metal-poor clusters tend to lie on the old-age model grid. This does imply some things for elliptical galaxies; however, if it were true, the galaxies would have such large numbers of stars in a spectroscopic aperture that stochastic fluctuations in AGB star activity would be minimal, so they would reach an average Hα and Hβ value with minimal scatter. The metal-rich portions of their stellar populations would contribute a partially infilled Balmer index series, and so the larger the percentage of their population that is metal rich, the younger they would appear in a Balmer–metal diagram. While something like this trend is seen observationally (Worthey et al. 1995) one should not jump to conclusions since even the higher-order Balmer features show a similar behavior.

3.5. Models

Are the line depths of current sets of models too deep? The Worthey models agree quite well with more modern model sets, especially after rescaling the ages by subtracting 2 Gyr. If, however, all authors are making the same mistake and all Balmer line strengths should be dropped to a level to make the low-lying globular clusters fit along the old-age sequence, then

there are some implications. First, even with correction for HB morphology, the metal-poor clusters will still look substantially younger. Second, the average elliptical galaxy will look young enough to raise eyebrows.

Despite this quandary, there may be one unlikely way to get the models to fit everything, or nearly everything, and that is to invoke hefty abundance ratio systematics, especially with oxygen and helium, that we could not test effectively in this paper. Such a scheme would require that element ratios drift in opposite directions for metal-rich globular clusters versus elliptical galaxies. The effects of O and He abundance would have operate mostly on the isochrone temperatures and age scales, and not operate significantly on the integrated stellar spectra. However, in the absence of more direct observational evidence, this scheme is very speculative.

4. CONCLUSION

Extracting information from the integrated light of stellar populations is not an easy process since there are many complex factors affecting the spectra. Decoupling the age–metallicity degeneracy by graphing Balmer line indices versus metal feature indices has allowed us to learn much more about stellar populations; however, the weakness of the observed Hβ line relative to the models needs to be explained. This paper shows that altered abundance ratios are unable to account for the observed weakness in the Balmer line strengths of globular clusters.

Of the other factors that can potentially affect the Balmer line strengths, HB morphology effects are hard to disentangle since they are also degenerate with age and metallicity, but seem well understood. By marking the clusters that have extended or blue HBs it becomes clear that HB morphology cannot solve the Hβ problem. Likewise, inclusion of blue stragglers will not help, even if there was evidence for a strong modulation of blue straggler frequency with metallicity, which there is not (Sandquist 2005). Emission fill-in of the Balmer lines due to hydrogen recombination lines from external nebulae is probably ruled out, except for case like the planetary nebula in M5. Stellar activity in individual cluster stars seems to be the only surviving mechanism that has good evidence. However, even being generous, the cool tail of M dwarfs does not appear to be able to generate enough flux to cause the modulation in Hβ needed. The remaining stellar source is flaring in M giants. These stars are bright enough, and inherently stochastic in nature, which seems to fit the observations of clusters that scatter to low Hβ rather randomly. Finally, it remains a long-shot possibility that abundance ratios in O or the noble gases can cause isochrone temperature drifts severe enough to affect the Hβ problem.

REFERENCES

Beasley, M. A., Brodie, J. P., Strader, J., Forbes, D. A., Proctor, R. N., Barmby, P., & Huchra, J. P. 2005, AJ, 129, 1412
Bica, E., & Alloin, D. 1986, A&A, 166, 83
Busso, G., et al. 2007, A&A, 474, 105
Cohen, J. G., Blakeslee, J. P., & Ryzhov, A. 1998, ApJ, 496, 808
Dotter, A., Chaboyer, B., Ferguson, J. W., Lee, H.-c., Worthey, G., Jevremović, D., & Baron, E. 2007, ApJ, 666, 403
Gratton, R., Sneden, C., & Carretta, E. 2004, ARA&A, 42, 385
Greggio, L., & Renzini, A. 1990, ApJ, 364, 35

Gunn, J. E., Stryker, L. L., & Tinsley, B. M. 1981, ApJ, 249, 48
Kafka, S., & Honeycutt, R. K. 2006, AJ, 132, 1517
Lee, H.-c., Yoon, S. -J., & Lee, Y. -W. 2000, AJ, 120, 998
Lee, H.-c., et al. 2009, ApJ, 694, 902
O'Connell, R. W. 1986, in Stellar Populations, ed. C. A. Norman, A. Renzini, & M. Tosi (Cambridge: Cambridge Univ. Press), 167
Osterbrock, D. A. 1989, Astrophysics of Gaseous Nebulae and Active Galactic Nuclei (Mill Valley, CA: Univ. Science Books)
Rabin, D. 1980, PhD thesis, California Institute of Technology
Rabin, D. 1982, ApJ, 261, 85
Sanches-Blazquez, P., et al. 2007, VizieR Online Data Catalog, 837, 10703
Sandquist, E. L. 2005, ApJ, 635, L73
Schiavon, R. P., Rose, J. A., Courteau, S., & MacArthur, L. A. 2004, ApJ, 608, 33
Schiavon, R. P., Rose, J. A., Courteau, S., & MacArthur, L. A. 2005, ApJS, 160, 163

Serven, J., Worthey, G., & Briley, M. M. 2005, ApJ, 627, 754
Trager, S. C., Worthey, G., Faber, S. M., Burstein, D., & Gonzalez, J. J. 1998, ApJS, 116, 1
Valdes, F., Gupta, R., Rose, J. A., Singh, H. P., & Bell, D. J. 2004, ApJS, 152, 251
West, A. A., Hawley, S. L., Bochanski, J. J., Covey, K. R., & Burgasser, A. J. 2010, in IAU Symp. 258, The Ages of Stars, ed. E. E. Mamajek, D. R. Soderblom, & R. F. G. Wyse (Cambridge: Cambridge Univ. Press), in press (arXiv:0812.1223)
Worthey, G. 1994, ApJS, 95, 107
Worthey, G., Faber, S. M., González, J. J., & Burnstein, D. 1994, ApJS, 94, 684
Worthey, G., & Ottaviani, D. L. 1997, ApJS, 111, 377
Worthey, G., Trager, S. C., & Faber, S. M. 1995, in ASP Conf. Ser. 86, Fresh Views of Elliptical Galaxies, ed. A. Buzzoni, A. Renzini, & A. Serrano (San Francisco, CA: ASP), 203